Soft Matter

View Online
Dynamic Article Links

Cite this: *Soft Matter*, 2011, **7**, 91

www.softmatter.org

PAPER

Langmuir–Blodgett assembly of bent-shaped rigid amphiphiles into spiral rings†

Libin Liu, Ho-Joong Kim and Myongsoo Lee*

Received 20th May 2010, Accepted 1st August 2010
DOI: 10.1039/c0sm00403k

We report here the interfacial behaviour and structure of the Langmuir–Blodgett films of a series of bent-shaped rigid amphiphiles. Molecule **1**, based on a shortest oligo(propylene oxide) chain, spontaneously aggregated into short cylinders at the air–water interface. Molecules **2** and **3** formed uniform monolayers at very low surface pressure. Upon compression nanorods appeared. Interestingly, these nanorods self-assemble into spiral rings nanostructures. High-resolution AFM images and UV-vis spectra with polarized light indicate that the nanorods, with a width of 5–8 nm and a length of 10–50 nm, were packed by 2–10 molecules *via* the π–π interaction of the rigid bent-core lying flat on the substrate. The spiral ring morphologies can be realized through a molecular design and a lateral compression. We suggested that the unusual spiral morphologies are associated with the peculiar rigid bent-shaped core and interfacial molecular interactions, such as capillary force and van der Waals attraction.

1. Introduction

Recently, nanomaterials with unique morphologies have received a great deal of attention due to their fascinating morphology-dependent properties.[1–3] Precise control of the morphologies with a well-defined shape and size is of critical importance. Such morphologically dependent properties play an important role in designing nanodevices. Therefore, several inorganic or hybrid organic–inorganic nanosystems have been investigated,[1,2] with far fewer examples based on organic nanomaterials.[4] In contrast to inorganic nanomaterials, organic systems are excellent candidates for nanodevices, owing to their electronic and optical properties, and flexibility in molecular design.[5] Bent-core molecules consisting of rigid rod and flexible coil segments, as a special kind of rigid-flexible block molecules, have been mainly studied in the mesomorphic phase.[6] Usually, organic functional materials have been processed in the form of films serving as active layers in devices; thus, studies of growth mechanism, molecular ordering, and the overall film morphology are of prime importance for device design.[7]

Herein, we report the self-assembly of bent-shaped rigid amphiphiles by using the Langmuir–Blodgett (LB) technique. Pressure induced 2-D spiral rings were observed, which consist of hundreds of molecular nanorods in a range of nanometre sizes. The inter-nanorod distances and the final superstructures can also be controlled by the compression process.

Center for Supramolecular Nano-Assembly, Department of Chemistry, Seoul National University, Seoul, 151-747, Korea. E-mail: myongslee@snu.ac.kr; Fax: +82 2 393 6096; Tel: +82 2 880 4340

† Electronic Supplementary Information (ESI) available: High resolution AFM images, polarized UV-vis. See DOI: 10.1039/c0sm00403k/

2. Experimental

2.1 Langmuir–Blodgett film fabrication

Langmuir isotherms at the air–water interface and Langmuir–Blodgett (LB) depositions onto a solid substrate were conducted at room temperature using a KSV 2000 LB minitrough. A 40–120 μL volume of dilute molecule solution (concentration less than 0.5 mg mL^{-1}) in chloroform (HPLC grade) was deposited in 5–10 drops, uniformly distributed onto the water surface (Nanopure, 18.2 MΩ cm) and left to evaporate and spread evenly over a period of 30 min. The limiting cross-sectional area was determined at the steep rise in the surface pressure related to the formation of the condensed monolayer. For the AFM measurement, the LB films of the molecules were transferred onto the substrates at various surface pressures by the upstroke mode of the vertical dipping method at a rate of 2 mm min^{-1} (if not indicated otherwise). For UV-vis measurements, the floating films were transferred onto quartz at selected surface pressure by the horizontal Langmuir–Schaefer method and by a certain number of depositions.

Highly polished [100] silicon wafers (Semiconductor Processing Co.) were cut into rectangular pieces (2 × 2 cm^2) and sonicated in Nanopure water for 10 min to remove silicon dust. The wafers were then chemically treated with "piranha solution" (30% concentrated hydrogen peroxide, 70% concentrated sulfuric acid, *hazardous solution*!) for 1 h and then washed copiously with Nanopure water.

2.2 Langmuir–Blodgett film characterization

The LB films on the silicon substrates were studied with a Nanoscope IIIa Multimode AFM. Scans were performed in the

"light" tapping mode in accordance with the usual procedure adopted in our laboratory.[8] Amplitude ratios of 0.95 and higher were employed to avoid damaging the films.[9] The domain topography and the surface area coverage were calculated from height histograms using the bearing analysis.[10] AFM characterization of the deposited LB films was done after drying in a desiccator for 24 h. The AFM scans were conducted at 0.5∼2 Hz scanning rate. The AFM tip radii were between 20 and 35 nm, and the spring constants of the cantilevers were in the range of 40–60 N m^{-1}. The AFM tip was evaluated by scanning a reference specimen of gold nanoparticles with a diameter of 3–5 nm, according to the known procedure.[11] The collected images were processed with either direct deconvolution of the tip shape by the mathematical morphology routine or with a simplified spherical approximation to deduce the tip radius (in the range of 5–10 nm). UV-vis measurements of the films were performed at room temperature using UV-1650PC spectrophotometer. A Glan–Taylor polarizer was set between the lamp and the sample to obtain the desired polarized UV-vis irradiation.

3. Results and discussion

The rigid amphiphiles consist of bent-shaped oligo(*p*-phenylene) and a oligo(propylene oxide) (OPO) chain at the bay position and were prepared as previously reported.[12] Molecule **1**, based on the shortest OPO chain, shows a steep rise in the surface pressure, indicating that the molecules with the shortest OPO chains do not provide stable amphiphilic behavior (Fig. 1). The AFM images of the film deposited on a piranha-treated silicon wafer, at the onset of the surface pressure, reveal short cylinders (Fig. 2a). The height of the cylinder is about 1.7 ± 0.2 nm and the width is about 23 ± 2 nm. Upon compression, the cylinders still keep their shape and are more densely packed (Fig. 2b and Fig. S1, ESI†). This is consistent with the isotherm data, which show the pressure monotonously increases, on the whole, as a result of crowding the aggregates. The formation of the cylinders is probably a result of the spontaneous aggregation which occurs whilst the samples spread on the water's surface.[13]

In contrast, molecule **2**, based on a longer OPO chain, reveals a steadily increasing surface pressure, indicating that the molecule displays stable amphiphilic behavior at the air–water interface (Fig. 1). The surface area occupied by the aromatic rod segments was calculated by the Corey–Pauling–Koltun (CPK) mode to be about 2.01 nm^2 in the flat-on orientation ($A_{rod//}$). The surface area of the OPO chains (A_{OPO}) was estimated by the area occupied by ethylene oxide chains (the methyl group would be exposed to air). The surface area of the ethylene oxide monomeric units oriented at the water surface and hydrogen-bonded

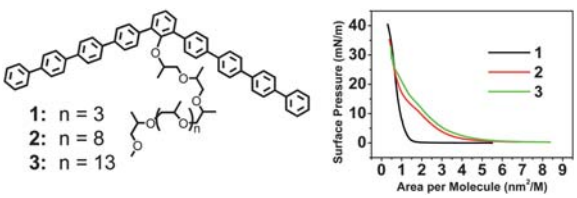

Fig. 1 (left) Molecular structures of **1**, **2**, **3**, and (right) their surface pressure–area (π–A) isotherms.

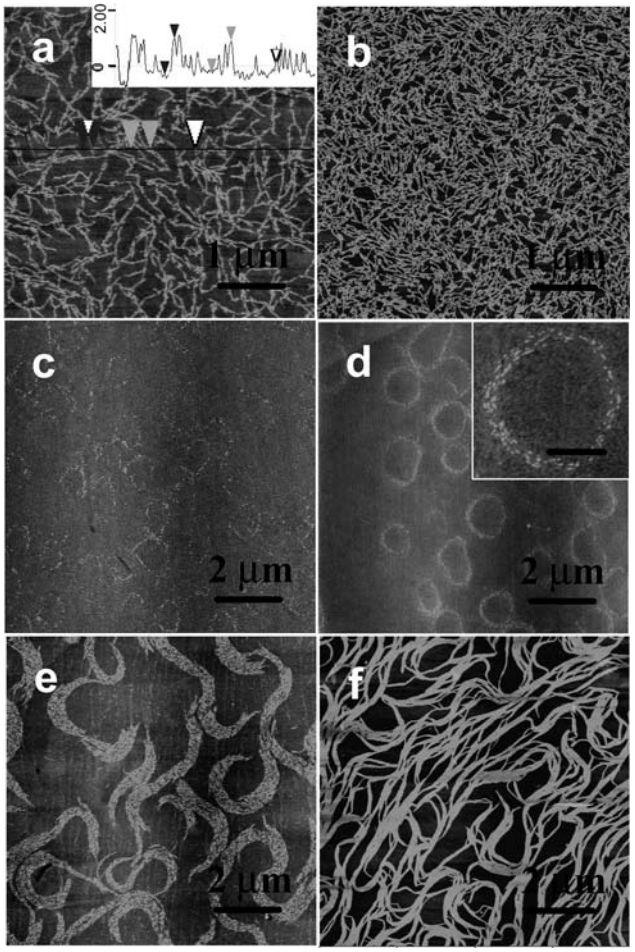

Fig. 2 AFM images of the LB films deposited onto piranha-treated silicon wafers. (a) At the onset of the surface pressure for **1**, (b) π = 10 mN m^{-1} for **1**, and (c) π = 0.5 mN m^{-1}, (d) π = 2 mN m^{-1}, (e) π = 5 mN m^{-1}, (f) π = 20 mN m^{-1} for **2**, *z* = 8 nm. Inset in (a) is the height profile and the high resolution AFM image is inserted in (d), scale bar: 500 nm.

with 1–3 water molecules is about 0.22–0.28 nm^2.[14] Therefore, the surface area occupied by a molecule is calculated as 4.64 nm^2 ($A_{rod//} + A_{OPO}$). By extrapolation of the slope of the curve to zero pressure, the limiting molecular area is about 4.32 nm^2, which is consistent with the area of the molecules flattened on the water's surface. The LB films deposited at the onset of the surface pressure (molecular area of 5.8 nm^2) show a uniform monolayer, with a surface microroughness of 0.3–0.5 nm (calculated within 1 × 1 μm^2), as expected for low-molecular-weight rod–coil molecules, as well as many flexible macromolecular materials.[15] Slightly compressed to 0.5 mN m^{-1}, the film shows the appearance of nanorods in the large area of the AFM images (Fig. 2c and Fig. S3, ESI†). The interesting point is that the nanorods seem to aggregate into a ring. Upon compression, more obvious spiral rings were clearly observed (Fig. 2d). The spiral rings covered all the 2 × 2 cm^2 piranha-treated silicon wafer's surface and a high film-transfer ratio (above 0.8) was observed, indicating that the morphology of the formed film at the air–water interface is preserved upon transfer.[16] High resolution AFM images indicate that the spiral rings were composed of hundreds of nanorods (Fig. 2d inset). Further compression leads the rings

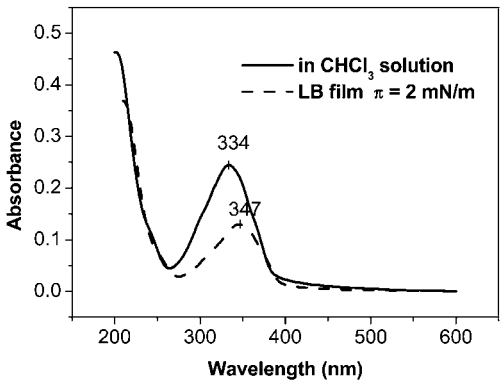

Fig. 3 UV-vis spectra of molecule **2** in $CHCl_3$ solution and the LB film deposited at a surface pressure of 2 mN m^{-1}.

to open to the spiral clusters (Fig. 2e). At this stage, the short rods can still preserve their identity. At 20 mN m^{-1}, the spiral clusters were connected to each other and the short rods were fused into long tapes (Fig. 2f).

The spiral rings only appeared at a low density liquid-like phase ($\pi < 5$ mN m^{-1}) (Fig. 2 and Fig. S4, ESI†). The UV-vis spectra of the LB films deposited at 2 mN m^{-1} were red shifted 13 nm compared to that of the chloroform solution, indicating the π–π interaction of molecules in the LB films[17] (Fig. 3). To further confirm the oligophenylene core orientation, polarized UV-vis spectroscopy was performed. When the film is investigated with polarized light, by using the light polarization plane, parallel (E_p) or perpendicular (E_s) to the incidence plane of radiation at an incidence angle $I = 0°$ of the light beam with respect to the plane normal, the main absorption features show a marked dependence on the direction of the electric field vector with respect to the dipping direction. However, in our case, no polarization dependence of the light absorption was observed (Fig. S5, ESI†). This is because the main absorption bands are polarized in the *xy* plane [the dichroic ratios $R = A(E_p)/A(E_s) = 1$ (A = absorbance)], which indicates that the oligophenylene core is flat on the quartz substrate.[18]

High-resolution images in the tapping mode at low forces revealed a dilated shape of the nanorods, which is a typical artifact produced by the AFM tip. We carefully analyzed the shape of these nanostructures with a very sharp carbon nanotube tip with a calibrated radius of less than 8 nm to deconvolute the tip shape and estimate the true lateral dimensions. We used hemispherical approximation to account for the tip dilation, in accordance with a known approach.[10] Considering the very small height of the nanostructure (analysis of 60 randomly selected cross sections of the nanorods in different spiral rings), tip dilation generally contributes less than 50% of the apparent lateral dimension, which makes the correction quite reliable. These results led us to the conclusion that the observed nanostructures are indeed nanorods with a width of 5–8 nm and a length of 10–50 nm, which were packed by 2–10 molecules *via* the π–π interaction of the rigid bent-core lying flat on the substrate, close to the molecular dimensions estimated from molecular models (Fig. 4). The nanorods should be a pre-organized monolayer of molecules and become more densely packed as the surface pressure increases. This reorganization can be related to the folding of the flexible tails and their dehydration due to expelling associated water molecules from the densely packed areas beneath the air–water interface.[19] The nanorods are well separated, which indicate a sufficient steric stabilization brought about by the OPO chains. The bulky flexible coils attached to the bent-core as side groups, would fill in the space and prohibit further aggregation of the nanorods. When deposited onto a substrate, OPO chains adsorb onto the hydrophilic surface underneath the hydrophobic backbone, which translates into increased thickness. The observed height of the superstructures was 1.5–1.9 nm.

It should be mentioned that the physical origin of the spiral rings differs significantly from that of the spiral nanostructures formed by barbituric acid, where the hydrogen bonding is responsible for the formation of the morphology.[20] In the present work, the spiral rings on the micrometre scale are composed of hundreds of molecular nanorods on the nanometre scale with an aspect ratio (length-to-width) of 2–10. Bates and Frenkel[21] have carried out Monte Carlo simulations on the phase behavior of 2D hard-rod systems with low aspect ratios. However, these simulations do not account for rod–rod directional interactions such as capillary force and van der Waals attraction. The molecular nanorods arranged in a parallel manner which may be due to two reasons, first, to maximize the entropy of the self-assembled structure of rodlike or nematic objects by minimizing the excluded volume per particle in the array, as first suggested by Onsager,[22] and second, because of the higher sum of van der Waals forces along the length of a nanorod as compared to its width.[23] The overall nematic-like arrangements are frequently disrupted by disclinations, which results in the spiral morphology.[24,25]

It is noticed that this type of morphology seldom occurs in nanorod systems, presumably because it is energetically unfavorable.[26] However, in our system the spiral rings composed of organic molecular nanorods are stable in a range of surface

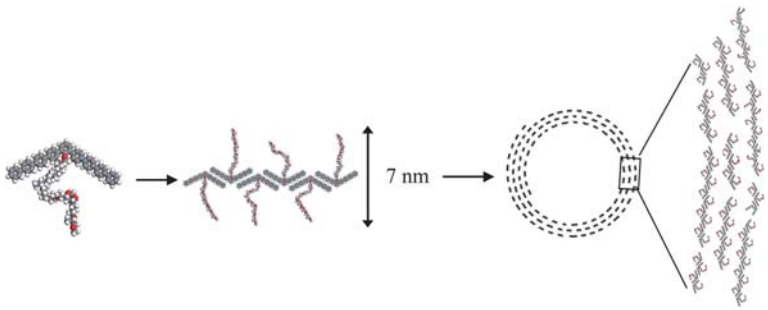

Fig. 4 A schematic representation of the spiral ring formed by the bent-core rigid amphiphiles.

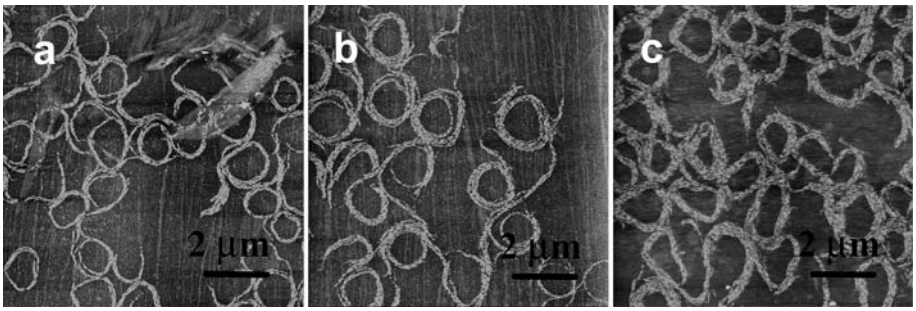

Fig. 5 The AFM images of spiral rings of **2** formed at $\pi = 2$ mN m^{-1} at different annealing times (a) 0.5 h, (b) 1 h, and (c) 2 h, $z = 8$ nm.

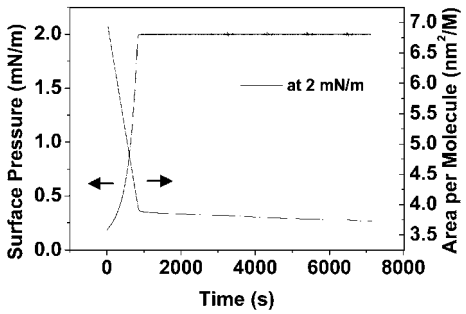

Fig. 6 The changes in surface area of **2** as a function of time and at a constant surface pressure of 2 mN m^{-1}.

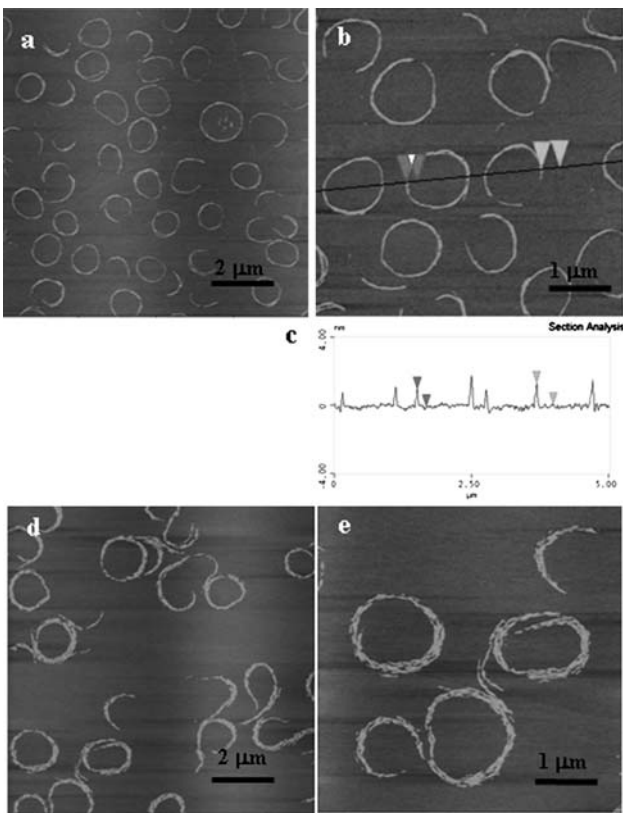

Fig. 7 The AFM images of **2** deposited on mica substrates at surface pressures of (a) and (b) 1 mN m^{-1}, (d) and (e) 3 mN m^{-1}, $z = 8$ nm. (c) is the height profile in (b).

pressure ($\pi < 5$ mN m^{-1}). When deposited at a rate of 40 mm min^{-1}, spiral rings were also observed (Fig. S6, ESI†). In addition, when the surface pressure was maintained at 2 mN m^{-1} for different times (annealing time) the width of the spiral changes. Additional nanorods were formed and joined the original spiral rings from the outside (Fig. 5). This was also reflected in the π–t or A–t isotherm data (Fig. 6). The film was compressed to a surface pressure of 2 mN m^{-1} and held constant at this value for a period of 120 min. The area per molecule decreased about 22 Å^2 over the 120 min period. This value corresponds to about 5% of the limiting molecular area of the monolayer.

To check the substrate effect on the spiral ring formation, the films were also deposited on the mica substrate. Spiral rings were also observed in the large molecular area range. (Fig. 7) When a mica substrate was used, a hydrophilic material with an advancing water contact angle of <10°, a thicker water layer must remain at the mica surface compared to that of piranha-treated silicon wafer (contact angle was found to be 26 ± 2°). It is quite reasonable to assume that such an intervening water layer masks the substrate's chemistry and enhances the molecular diffusion and mobility, thereby promoting more efficient self-organization of the molecules in the nanorods. This is why the size of the ring seems to be more uniform and the short rods are more densely packed on mica substrates (Fig. 7).

4. Conclusions

To get a general conclusion, molecule **3**, based on the longest OPO chain, was also investigated, which shows a similar isotherm curve to that of **2** where only larger molecular areas were occupied due to the longer OPO chain (Fig. 1). When the films were deposited on the solid substrate, spiral rings were also observed (Fig. S7, ESI†). We would like to conclude that, for the spiral ring formation of the organic molecules, two conditions must be satisfied: (i) a core with low aspect ratios that is sufficiently rigid that entropy minimization will align molecules when they densely pack (ii) side chains must be sufficiently long and flexible to fluidize dense-packed states. We expect that the molecular ordering of the spiral rings could be used as active layers in devices. The bending angle of the bent-shaped molecules is very important for molecular assembly,[27] further studies on potential optoelectronic functions of the conjugated core of the molecules, and the effect of the bending angle on morphology, are needed.

Acknowledgements

We gratefully acknowledge the National Creative Research Initiative Program of the Korean Ministry of Science and Technology for financially supporting this work.

Notes and references

1 (*a*) M. A. El-Sayed, *Acc. Chem. Res.*, 2001, **34**, 257; (*b*) G. R. Patzke, F. Krumeich and R. Nesper, *Angew. Chem., Int. Ed.*, 2002, **41**, 2446; (*c*) Y. Xia, P. Yang, Y. Sun, Y. Wu, B. Mayers, B. Gates, Y. Yin, F. Kim and H. Yan, *Adv. Mater.*, 2003, **15**, 353.
2 (*a*) S. J. Hurst, E. K. Payne, L. Qin and C. A. Mirkin, *Angew. Chem., Int. Ed.*, 2006, **45**, 2672; (*b*) X. Li, L. Zhang, X. Wang, I. Shimoyama, X. Sun, W. Seo and H. Dai, *J. Am. Chem. Soc.*, 2007, **129**, 4890.
3 (*a*) J.-H. Ryu, D.-J. Hong and M. Lee, *Chem. Commun.*, 2008, 1043; (*b*) L. Liu, K.-S. Moon, R. Gunawidjaja, E. Lee, V. V. Tsukruk and M. Lee, *Langmuir*, 2008, **24**, 3930; (*c*) L. Liu, D.-J. Hong and M. Lee, *Langmuir*, 2009, **25**, 5061.
4 N. Reitzel, T. Hassenkam, K. Balashev, T. R. Jensen, P. B. Howes, K. Kjaer, A. Fechtenkötter, N. Tchebotareva, S. Ito, K. Müllen and T. Bjørnholm, *Chem.–Eur. J.*, 2001, **7**, 4894.
5 (*a*) L. Jiang, Y. Fu, H. Li and W. Hu, *J. Am. Chem. Soc.*, 2008, **130**, 3937; (*b*) Y. Che, A. Datar, K. Balakrishnan and L. Zang, *J. Am. Chem. Soc.*, 2007, **129**, 7234; (*c*) M. L. Tang, A. D. Reichardt, N. Mikayi, R. M. Stoltenberg and Z. Bao, *J. Am. Chem. Soc.*, 2008, **130**, 6064.
6 (*a*) R. A. Reddy, U. Baumeister and C. Tschierske, *Chem. Commun.*, 2009, 4236; (*b*) J. Etxebarria and M. B. Ros, *J. Mater. Chem.*, 2008, **18**, 2919.
7 (*a*) A. Jákli, D. Krüerke and G. G. Nair, *Phys. Rev. E: Stat., Nonlinear, Soft Matter Phys.*, 2003, **67**, 051702; (*b*) A. Jákli, D. Krüerke, H. Sawade, L. C. Chien and G. Heppke, *Liq. Cryst.*, 2002, **29**, 377.
8 V. V. Tsukruk and D. H. Reneker, *Polymer*, 1995, **36**, 1791.
9 S. N. Magonov, V. Elings and M. H. Whangbo, *Surf. Sci.*, 1997, **375**, L385.
10 S. N. Magonov, *Surface Analysis with STM and AFM: experiment and theoretical aspects of image analysis*; VCH: New York, 1996.
11 V. V. Tsukruk, *Rubber Chem. Techn.*, 1997, **70**, 430.
12 H.-J. Kim, Y.-H. Jeong, E. Lee and M. Lee, *J. Am. Chem. Soc.*, 2009, **131**, 17371.
13 (*a*) J. K. Cox, K. Yu, B. Constantine, A. Eisenberg and R. B. Lennox, *Langmuir*, 1999, **15**, 7714; (*b*) L. Liu, J.-K. Kim and M. Lee, *ChemPhysChem*, 2008, **9**, 1585.
14 (*a*) J. K. Cox, K. Yu, A. Eisenberg and R. B. Lennox, *Phys. Chem. Chem. Phys.*, 1999, **1**, 4417; (*b*) M. C. Fauré, P. Bassereau, M. A. Carignano, I. Szleifer, Y. Gallot and D. Andelman, *Eur. Phys. J. B*, 1998, **3**, 365.
15 (*a*) L. Liu, J.-K. Kim, R. Gunawidjaja, V. V. Tsukruk and M. Lee, *Langmuir*, 2008, **24**, 12340; (*b*) S. Peleshanko, R. Gunawidjaja, S. Petrash and V. V. Tsukruk, *Macromolecules*, 2006, **39**, 4756.
16 (*a*) K. L. Genson, D. Vaknin, O. Villacencio, D. V. McGrath and V. V. Tsukruk, *J. Phys. Chem. B*, 2002, **106**, 11277; (*b*) H. Riegler and K. Spratte, *Thin Solid Films*, 1992, **210–211**, 9.
17 (*a*) J. Kim and T. M. Swager, *Nature*, 2001, **411**, 1030; (*b*) J. Kim, I. A. Levitsky, D. T. McQuade and T. M. Swager, *J. Am. Chem. Soc.*, 2002, **124**, 7710.
18 G. Ricciardi, S. Belviso, G. Giancane, R. Tafuro, T. Wagner and L. Valli, *J. Phys. Chem. B*, 2004, **108**, 7854.
19 Z. Xu, N. B. Holland and R. E. Marchant, *Langmuir*, 2001, **17**, 377.
20 X. Huang, C. Li, S. Jiang, X. Wang, B. Zhang and M. Liu, *J. Am. Chem. Soc.*, 2004, **126**, 1322.
21 M. A. Bates and D. Frenkel, *J. Chem. Phys.*, 2000, **112**, 10034.
22 L. Onsager, *Ann. N. Y. Acad. Sci.*, 1949, **51**, 627.
23 B. Nikoobakht, Z. L. Wang and M. A. El-Sayed, *J. Phys. Chem. B*, 2000, **104**, 8635.
24 C. Messerschmidt, A. Schulz, J. Zimmermann and J. Fuhrhop, *Langmuir*, 2000, **16**, 5790.
25 *Points, Linkes and walls in liquid crustals, magnetic systems and various ordered media*, Ed. M. Kleman, John Wiley & Sons: New York, 1983.
26 F. Kim, S. Kwan, J. Akana and P. Yang, *J. Am. Chem. Soc.*, 2001, **123**, 4360.
27 (*a*) A. Dewar and P. J. Camp, *Phys. Rev. E: Stat., Nonlinear, Soft Matter Phys.*, 2004, **70**, 011704; (*b*) C. Bailey and A. Jákli, *Phys. Rev. Lett.*, 2007, **99**, 207801.